Fluids and Barriers of the CNS

RESEARCH

Open Access

Neurogenesis and glial impairments in congenital hydrocephalus: insights from a BioGlue-induced fetal lamb model

Dicle Karakaya[1,2], Kristin Lampe[1], Jose L. Encinas[3], Soner Duru[1], Lucas Peiro[1], Halil Kamil Oge[2], Francisco M. Sanchez-Margallo[4], Marc Oria[1,5,6,7†] and Jose L. Peiro[1,8*†]

Abstract

Background Congenital hydrocephalus (HCP) is a prevalent condition, that leads to fetal cerebral ventricle dilation and increased intracranial pressure. It is associated with significant neurological impairments, partly due to the disruption of neurogenesis and gliogenesis. This study aims to investigate alterations in the proliferation and differentiation of neural progenitor cells (NPCs) in a fetal lamb model of obstructive HCP induced by intracisternal BioGlue injection, to identify the potential optimal intervention time for prenatal surgery.

Methods This study involved 22 fetal lambs, divided into control (n = 10) and HCP (n = 12) groups with hydrocephalus induced at approximately 85–90 gestational days. Histological and molecular techniques, including hematoxylin and eosin staining, triple immunofluorescence, Western blot analysis, and RT-qPCR, were utilized to assess changes in NPCs, astrocytes, and oligodendrocytes across three different gestational stages (E105, E125, and E140). The analysis of data was done by using multiple (unpaired) two-sample t-test and was represented as mean and standard deviation.

Results HCP led to significant disruptions in the ventricular zone (VZ), with the translocation of NPCs into the intraventricular CSF and formation of periventricular heterotopias. This study revealed an initial surge in the expression of NPC markers (Pax6 and Sox2), which decreased as HCP progressed. Astroglia reaction intensified, as indicated by increased expression of GFAP, vimentin, and aquaporin 4, particularly at later stages of pregnancy ($p < 0.001$, $p < 0.001$ and $p < 0.001$, control and HCP E140, respectively). Myelin formation was also adversely affected, with reduced expression of oligodendrocyte markers (Olig2 and Sox10, $p = 0.01$ and $p = 0.009$, control and HCP E140, respectively) and myelin proteins (MOBP, MOG and MBP, $p = 0.02$, $p = 0.049$ and $p = 0.02$ control and HCP E140, respectively).

Conclusions This study contributed to clarify the profound impact of congenital HCP on neurogenesis and gliogenesis in an experimental fetal lamb model. The VZ disruption and altered expression of key neurogenic and glial markers suggested a significant pathological process underlying neurodevelopmental abnormalities. The findings suggested a potential window for prenatal surgical intervention between E105 and E125 in the sheep model, offering new avenues for prenatal therapeutic approaches and improving surgical outcomes in affected fetuses and neonates.

Keywords Congenital hydrocephalus, Gliogenesis, Neurogenesis, Neural progenitor cells, Prenatal surgery

†Marc Oria and Jose L. Peiro have equal responsibility for all aspects of this publication.

*Correspondence:
Jose L. Peiro
Jose.Peiro@cchmc.org
Full list of author information is available at the end of the article

Background

Congenital hydrocephalus (HCP), characterized by the excessive accumulation of cerebrospinal fluid (CSF), leads to the dilation of ventricles and increased intracranial pressure [1] secondary to the obstruction of the system. It is a multifactorial disease that can initiate during the early embryonic development. It is one of the most common congenital anomalies, with an incidence ranging from 1 to 3 per 1000 live births, and it constitutes the primary indication for pediatric neurosurgical interventions [1]. HCP that onsets during fetal, perinatal, or neonatal stages tends to be more challenging to treat and often leads to unfavorable neurological outcomes [1]. The severity of damage and prognosis depend on the underlying cause of hydrocephalus, associated malformations, age at onset, and timing and success of surgical intervention [2, 3].

It is crucial to know that hydrocephalus represents more than just a disorder related to CSF dynamics; it significantly affects the brain parenchyma development, so surgical interventions may not address all aspects of this condition [4–6]. In many shunted hydrocephalic children, neurological impairments cannot be reversed and ventriculomegaly often persists [7, 8]. There is also evidence suggesting that congenital hydrocephalus and disorders of brain maldevelopment with abnormal neurogenesis share common mechanisms and etiologies, such as cell junction pathologies and mutations in pathways involved in cell proliferation and growth [9–11].

Fetal hydrocephalus is also associated with alterations in the ependymal cells and lining, that lead to ependymal loss/denudation at the cerebral ventricles and aqueduct [12, 13]. This disruption starts around the 16th to 17th gestational week [14] in the telencephalon and continues throughout pregnancy, following both spatial and temporal patterns from caudal to rostral causing severe damage [9, 10, 13, 15, 16]. Denudation of the telencephalic ventricular zone (VZ) leads to abnormal neurogenesis, resulting in the translocation of neural progenitor cells (NPCs) into the CSF, the formation of subependymal rosettes, and the development of periventricular heterotopia, which is considered the focus of epilepsy observed in hydrocephalic patients [9, 17].

Furthermore, neuroinflammation has been proposed as a significant factor contributing to the progression of HCP, characterized by activation of microglia and astrocytes which are critical in the inflammatory response within the brain [1, 18]. These glial cells release various cytokines and chemokines that can exacerbate brain injury by promoting further inflammation and contributing to neuronal and axonal damage. Research indicates that the rise in intracranial pressure due to hydrocephalus correlates with the onset of gliosis, and that the shunt placement, regardless of duration, results in a decrease in both astrocytic and microglial reaction [19]. Concurrently, dysmyelination occurs as the oligodendrocytes, which are responsible for myelin formation, become impaired. All these findings are complemented by the recent study by Bonilla G et al., who have demonstrated astrocyte and microglial activation leading to neuroinflammation with a decrease of oligodendrocytes and progenitors kaolin-induced hydrocephalus model in juvenile pigs [20].

Numerous studies have demonstrated how changes manifest in animal models, detailing cellular mechanisms such as the stenosis of cerebral aqueducts [9, 13], protein overexpression in ependymal cells [21], microglial response [22] and neuronal and oligodendrocyte loss [23]. Further experimental insights from Del Bigio MR and Zhang YW [15, 24] along with Jimenez AJ et al. [16] have explored the pathophysiological consequences of hydrocephalus, revealing degenerative and proliferative brain changes in kaolin-induced hydrocephalus models and in hyh mutant mice, respectively. Clinical observations also corroborate these findings. They provide direct observations from human cases, documenting neuroependymal denudation in premature neonates with intraventricular hemorrhage [25] and full-term human fetal spina bifida aperta [12], and linking cell junction pathology to ventricular zone disruption in hydrocephalic patients [17]. Together, these studies bridge experimental models and clinical observations, presenting a comprehensive view of the developmental and pathological progression of fetal hydrocephalus from both perspectives.

The aim of this study was to determine the proliferation and differentiation of NPCs into immature neural cells, astrocytes, and oligodendrocytes in the subventricular zone. Moreover, to compare their changes at different intrauterine stages to finally predict the appropriate time point for an eventual therapeutic fetal intervention in an experimental fetal obstructive hydrocephalus sheep model.

Methods

Animal groups and BioGlue-induced fetal lamb obstructive HCP model

A total of 12 pregnant ewes with age less than 2 years old were used in this study. Among them, 10 ewes had twin pregnancies, totaling 22 fetal lambs. In twin pregnancies, HCP was induced in one fetus by injecting BioGlue, while the other twin fetus was maintained as a control and no injections were administered for reducing the number of sheep and surgical risks such as fetal loss.The experiments followed the guidelines for animal research and were approved by the Institutional Animal Care and Use Committee (IACUC: ES100370001499) at the Jesus Uson

Minimally Invasive Surgery Centre, Caceres, Spain and by the Institutional Animal Care and Use Committee at Cincinnati Children's Hospital Medical Center (IACUC 2021–0008), Cincinnati, Ohio, USA.

All young pregnant mothers were housed in groups under standard housing conditions at constant temperature (22 ± 1 °C) and humidity (30–55%) with a standard 12-h light/dark cycle. They were fed standard sheep chow and unlimited access to water (ad libitum) was provided.

The animal model was based on a previously described by Oria et al. and conducted at the Cincinnati Children's Hospital [26, 27]. Surgical procedures were performed under sterile conditions at approximately 85–90 gestational days (E85-90), during the second trimester of pregnancy. The ewes were fasted for 12 h prior to surgery but had ad libitum access to water. Sedation was induced using intravenous ketamine (10 mg/kg) and midazolam (0.3–0.5 mg/kg), followed by the administration of 2–3% isoflurane via an endotracheal tube, with oxygen, using mechanical ventilation. Approximately 30 min before surgery, the sheep received 1 g of cefazolin intravenously, and, for pain control, each animal was administered 0.005 mg/kg of buprenorphine (intramuscularly). The uterus was externalized, and after manually stabilizing the fetal head, a 22-gauge catheter needle was directed upwards at a 45-degree angle through the transuterine route, entering the subarachnoid space from the caudal aspect of the external occipital protuberance. Approximately 1.5 mL of cerebrospinal fluid (equal to the injection volume) was aspirated and then 1.5 mL of sterile BioGlue (consisting of purified bovine albumin and glutaraldehyde) was slowly injected into the cisterna magna. To reduce the volume of BioGlue to 1.5 mL was based on our observations from earlier studies where 2.0 and 2.5 mL of BioGlue led to severe and acute hydrocephalus [26]. Our aim was to diminish the severity and rapid progression of hydrocephalus, enabling a more detailed investigation into its chronic development and reducing fetal loss. After the transuterine injection, the maternal abdominal wall and skin were closed in a layered fashion.

To better understand the timeline of experimental design and pathological changes in this study, it is important to compare the gestational periods of sheep and humans and align their respective developmental stages. Fetal lambs have a gestational period of approximately 145 to 150 days, while human gestation lasts about 280 days. Key developmental milestones are relatively comparable; day 45–50 in sheep corresponds to the end of the first trimester in humans, day 85–90 in sheep approximates the mid-second trimester [26], and day 120–125 matches the late second trimester-early third trimester in humans. Full term for sheep, around day 145–150, parallels full-term human gestation. This comparison allows researchers and clinicians to correlate developmental changes and potential interventions across species, particularly studies on prenatal medicine, fetal surgery, and developmental biology.

The following groups were divided randomly and examined at three gestational ages (E105, E125, and E140):

1. Control: non-affected fetal brains ($n = 3–4$ for each time point).
2. HCP: fetal brains with BioGlue-induced hydrocephalus ($n = 3–4$ for each time point).

These groups were formed to investigate and compare developmental and hydrocephalus-related changes across different time-points of fetal development. Cesarean sections were performed at approximately E105, E125 and E140 under maternal anesthesia and then, sheep were euthanized with intravenous pentobarbital sodium (1 cc/4.5 kg).

Morphological and histological examination

Fetal brains were extracted, with one hemisphere being preserved in formalin for histopathological investigations, and the other half was sectioned and frozen at −80 °C for molecular studies.

Half of each brain was kept in formalin for 48 h and embedded in a paraffin block using a Leica Eg1150H system, following a series of washes with 70% alcohol. Then, the blocks were sectioned into 5-µm slices, encompassing the periventricular region. These sections were further processed according to the standard protocol for hematoxylin and eosin (H&E) staining.

Immunostaining

To identify NPCs, brain tissue sections were stained with primary antibodies against Pax6 (Abcam, ab5790, 1:50) and Sox2 (NovusBio, NB110-37235, 1:200). To label astrocytes, primary antibodies targeting GFAP (glial fibrillary acidic protein) (NovusBio, NBP1-05198, 1:1000) and vimentin (Sigma, V6630, 1:50) were used. Both proteins are intermediate filament proteins found in astrocytes [28]. And lastly, Olig2 (Millipore, ABE1024, 1:250), a transcription factor that activates genes associated with myelination in oligodendrocytes, and MBP (myelin basic protein) (AvesLab, MBP89927985, 1:100) were used as markers of the oligodendrocytes and formation of myelin [29].

For immunofluorescence staining, after deparaffinization of the sections, the slides were placed in a pressure cooker on high pressure at 114 °C-121 °C in 10 mM pH 6 sodium citrate buffer during 15 min for heat-mediated antigen retrieval, and then incubated at room

temperature (RT) for 25–30 min. Following cooling, the sections were incubated with 0.1% Triton X-100 (Sigma Aldrich) in phosphate-buffered saline (PBS) for 10 min at RT to permeabilize the cells. All samples were washed with PBS and incubated with a blocking solution (1% bovine serum albumin (BSA), 10% normal goat serum, 0.1% Triton X-100, and 0.05% Tween-20 in PBS) for 1 h.

The sections were then incubated overnight at 4 °C in a humid chamber with the primary antibodies mentioned previously. Sections were washed and incubated for 1 h at RT with secondary antibodies (Alexa Fluor 488-conjugated goat anti-rabbit IgG secondary antibody, 1:1000; Alexa Fluor 568-conjugated goat anti-mouse IgG secondary antibody, 1:1000; Alexa Fluor 647-conjugated goat anti-chicken or goat anti-guinea pig IgG secondary antibody, 1:500; Thermo Fisher Scientific), and DAPI (1:4000) was used to stain DNA, making the nuclei visible. To remove unwanted autofluorescence, Vector TrueVIEW Autofluorescence Quenching Kit (SP-8400-15, Vector Laboratories) was used to perform "Quenching" before cover-slipping with Prolong Diamond anti-fade mounting media (Thermo Fisher Scientific, P36961) and visualized with a Nikon fluorescence microscope (Nikon Inc.).

Two different triple immunofluorescence staining (Pax6-GFAP-Olig2 and Sox2-Vimentin-MBP) were applied to identify NPCs, astrocytes, and oligodendrocytes/myelin distribution.

Western blot analysis

Total protein isolation was carried out using homogenization in N-PER buffer (Neuronal Protein Extraction Reagent, Thermo Scientific) with protease and phosphatase inhibitor cocktails. Protein quantification was performed using the Pierce™ BCA Protein Assay Kit (Thermo Scientific).

Western blot analysis was subsequently conducted for Pax6, Sox2, GFAP, Vimentin, Olig2, MBP and doublecortin (DCX). Blots were treated with primary antibodies against Pax6 (Abcam, ab5790, 1:1000), Sox2 (NovusBio, NB110-37235, 1:2000), GFAP (NovusBio, NBP1-05198, 1:5000), Vimentin (Sigma, V6630, 1:200), Olig2 (Millipore, ABE1024, 1:1000), MBP (AvesLab, MBP89927985, 1:2000) and DCX (Invitrogen, PA5-17428, 1:1000) overnight at + 4 °C, followed by a one-hour treatment with secondary antibodies (anti-rabbit IgG HRP-linked, Cell Signaling Technology, 7074S, 1:1000; anti-mouse IgG HRP-linked, Cell Signaling Technology, 7076S, 1:1000; donkey anti-chicken IgY H&L (HRP), Abcam, ab16349, 1:2000 and goat anti-Guinea pig IgG H&L (HRP), Abcam, ab97155, 1:10000) at room temperature. Beta-actin (mouse, Abcam, ab8226, 1:1000, and rabbit, Cell Signaling Technology, 4970S, 1:1000) was used as a reference protein. To estimate the sizes of the bands, a biotinylated protein ladder (Cell Signaling Technology, 81851S) and anti-biotin HRP-linked antibody (Cell Signaling Technology, 7075P5, 1:1000) were used. Chemiluminescent imaging was performed using a Bio-Rad ChemiDoc MP (Bio-Rad) with either PierceTM ECL Western Blotting Substrate or SuperSignalTM West Femto Maximum Sensitivity Substrate.

RNA extraction and RT-qPCR analysis

Frozen brain tissues were transferred to 2 ml microcentrifuge tubes, and 1 ml of TRIzol was added to each tube. Using a Qiagen dispenser, a ball bearing was added to each sample tube, and the samples were homogenized for 2–5 min at 30 Hz in a Qiagen TissueLyserII homogenizer. For phase separation, 200 µl of chloroform was added, the mixture was incubated at RT for 5 min, and the samples were centrifuged at 12000xg at 4 °C. The upper liquid layer was transferred to a clean tube, and RNA was precipitated by adding 500 µl of isopropanol. After pipetting, the mixture was incubated at RT for 15 min. To form a gel-like pellet, the samples were centrifuged at 12000xg for 10 min at 4 °C. After discarding the supernatant, the pellets were washed with 1 mL of DEPC-treated water containing 75% ethanol, vortexed, and then centrifuged at 7500xg for 5 min at 4 °C. This step was repeated once more, and after removing the 75% ethanol, the RNA was air-dried and then dissolved in 50–100 µl of RNase-free water. RNA quantity and quality were assessed using an Epoch BioTek Synergy spectrophotometer (Biotek Instruments, Winooski, VT, United States), considering the A260 and A260/A280 values.

A 1 µg RNA/sample was reverse transcribed into complementary DNA (cDNA) utilizing the Qiagen RT^2 First Strand Kit (Qiagen Sciences, MD, United States) following the manufacturer's protocol and then used as a template for RT-qPCR employing TaqMan® gene expression assays (Applied Biosystems, Foster City, CA, United States). RT-qPCR was performed using cDNA samples, Taqman™ Master Mix (Thermo Fisher Scientific) and species-specific probes for sheep. Samples were run in duplicate for target genes and normalized using HPRT1 as the endogenous control. Relative quantification of transcript expression was carried out using the $2^{-\Delta\Delta Ct}$ method, where Ct represents the threshold cycle.

Samples underwent duplicate runs for target genes and were normalized using HPRT1 as the endogenous control. Relative quantification of transcript expression was conducted using the $2^{-\Delta\Delta Ct}$ method, with Ct representing the threshold cycle.

Statistical analysis

The data are represented as mean and standard deviation, unless otherwise specified. A p-value < 0.05 was considered statistically significant. To evaluate the statistical significance of differences between experimental groups Control vs HCP, a multiple (unpaired) two-sample t-test was conducted for normally distributed continuous data (Additional file 1). Prior to performing the t-test, the assumption of normality was assessed using the Shapiro–Wilk test in Control and HCP groups. Graphical and statistical computations were performed using the GraphPad Prism 10 software package.

Results

VZ disruption leads to translocation of NSCs/NPCs into CSF and PH formation

After HCP induction during E85-90 days, disruption of the VZ (also called ependymal denudation) was observed around the ventricles starting at E105 throughout all time periods. SVZ cells located at these denudation foci were the subjects of analysis in this research for understanding the pathology.

There is evidence that ependymal denudation leads to various neuropathological events, including the formation of periventricular heterotopia and subependymal rosettes, and the translocation of NSCs/NPCs to the CSF, suggesting a link between VZ disruption and abnormal cortical organization and function [9, 17]. H&E and immunofluorescence staining's showed that neural progenitors exposed at the surface of the disrupted VZ and displaced into the ventricle. In areas where NSCs/NPCs have been lost due to VZ disruption results in the accumulation of arrested neuroblasts produced in the SVZ in periventricular areas, contributing to the formation of PH (Fig. 1).

Disrupted VZ results in reduction of neural precursor cells

Neurogenesis in the developing brain involves complex interactions between different progenitor cell types and transcription factors that regulate their differentiation and fate. The expression of specific markers like Sox2, Pax6, and Tbr2 is essential for controlling the proliferation and differentiation of these progenitor cells [30]. Pax6 is critical for the development of the central

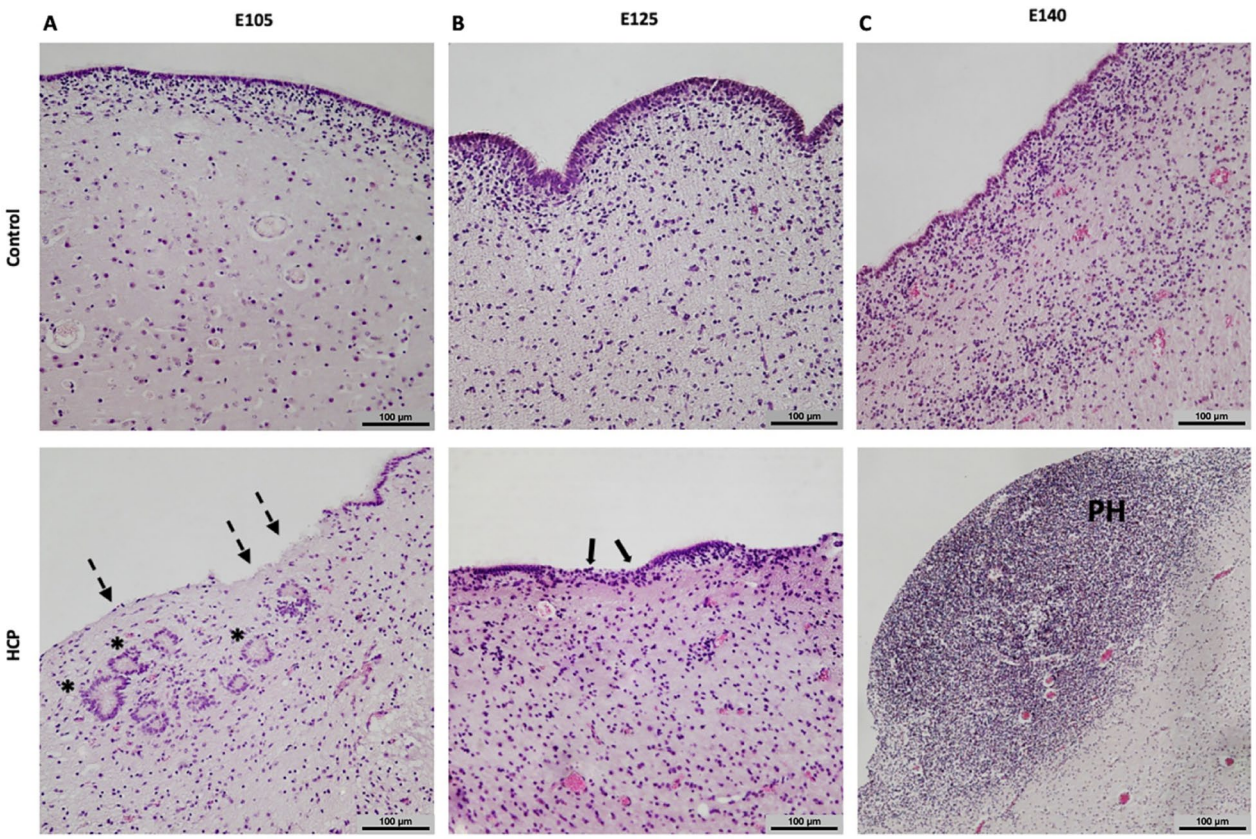

Fig. 1 Histopathological findings with H&E staining. Disruption of the VZ results in abnormalities in neurogenesis. **A** E105-HCP: Periventricular region of a hydrocephalic fetus at E105 with a large denuded area (broken arrows) and subependymal rosettes (asterisk). **B** E125-HCP: Translocation of NSCs/NPCs to the CSF (full arrows). **C** E140-HCP: Periventricular heterotopia formation (× 10, scale bar 100 µm)

nervous system. Its expression is observed in neuroepithelial (NECs) and radial glial cells (RGCs), which have the capacity to give rise to neural stem cells (NSCs). Recent research has shown the various functions of Pax6, including its involvement in maintaining the NSC population, regulating both embryonic and adult neurogenesis, contributing to brain modeling, facilitating neuronal migration, and participating in the formation of neural circuits [31]. Likewise, Sox2 is a transcription factor associated with the self-renewal of NPCs and shares functional similarities with Pax6 [32].

Consistent with these insights, one aspect of the current study was to investigate the distribution of NPCs throughout fetal development in the cases of HCP. At the onset of gestation (E105), immunofluorescence staining revealed an initial surge in Pax6 and Sox2-positive cells, which gradually declined as pregnancy progressed (Figs. 2D, 3D). These findings in early-stage hydrocephalic samples (E105) were supported by both Pax6 and Sox2 gene and protein expressions, which displayed an increase compared to those in control group, although the differences were not statistically significant. Nonetheless, with the progression of gestation, Pax6 and Sox2 expression gradually increased until E140 in the control group compared to the E105 and E125 groups, while a decrease in Pax6 expression was observed in the HCP groups, albeit not statistically significant. Notably, a remarkable downregulation of Sox2 was observed at E125 and E140 compared to the control groups ($p=0.002$ and $p<0.001$, control and HCP E125 and E140, respectively) (Figs. 2A, 3A).

Ependymal denudation causes alterations in neurogenesis

Next, we aimed to investigate how changes in other transcription factors, including Tbr2, Ascl1, and DCX are implicated in neuronal differentiation and migration during subsequent stages of pregnancy under both normal conditions and in the presence of HCP.

Distinct transcription factor sequences, such as Pax6 → Ngn2 → Tbr2 → Tbr1, coordinate the differentiation of radial glia to basal intermediate progenitors (bIPs) and subsequently to postmitotic projection neurons [33, 34]. Tbr2 acts as a key regulator of bIP identification and biogenesis [35–37], influencing the generation of glutamatergic projection neurons while suppressing alternative neural fates in the cerebral cortex [37], whereas Ascl1 (also called Mash1) promotes GABAergic interneurons [36, 38], with GABAergic differentiation

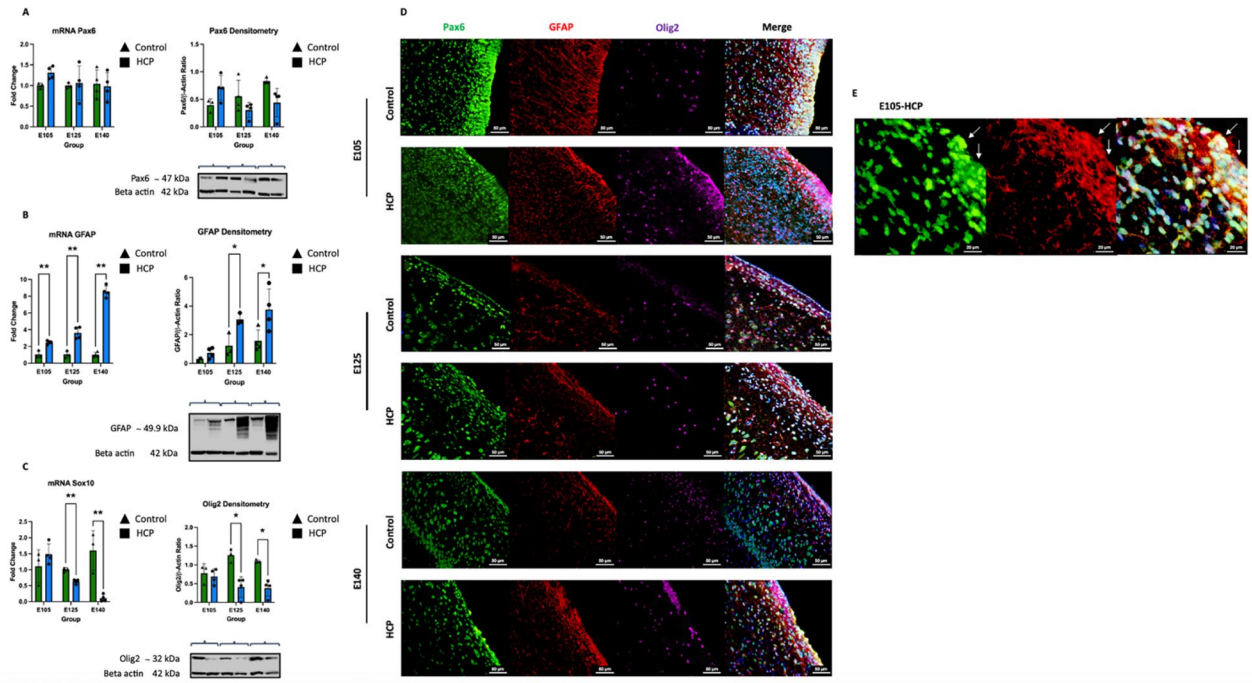

Fig. 2 Expressions and distributions of Pax6, GFAP, Olig2 and Sox10 in HCP. **A** Pax6 gene and protein expressions increased in HCP compared with control brain tissue at E105. As gestation progressed, its expression decreased gradually. **B** From the early stages of HCP, significant increase in GFAP relative expression were observed. Western blot analysis also confirmed higher protein levels of GFAP in the hydrocephalic groups, indicating an enhanced astroglial response to HCP. **C** Sox10 relative gene expression and Olig2 protein level downregulated starting from E125 (Data in the bar graphs represent mean ± SEM, green bars: control, blue bars: HCP) (*$p<0.05$, **$p<0.01$). D) Immunostainings of Pax6 (green), GFAP (red), Olig2 (magenta) and DAPI in control and hydrocephalic brains at three gestational ages E105, E125 and E140 (×20, scale bar 50 µm). **E** Pax6 (green) and GFAP (red) reactive NPCs exhibited co-expression (yellow) at E105 in HCP (white arrows) (×40, scale bar 20 µm)

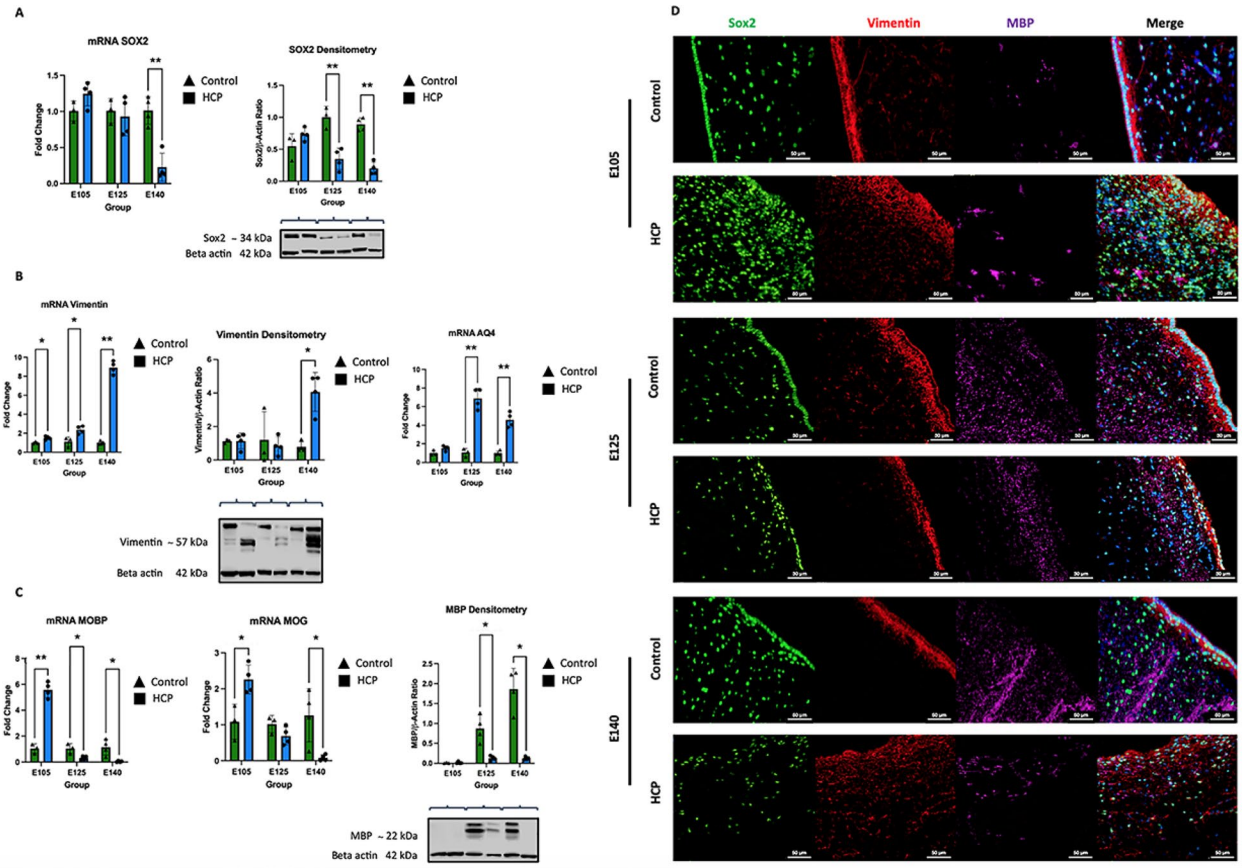

Fig. 3 Expressions and distributions of Sox2, Vimentin, Aq4, MOBP, MOG and MBP in HCP. **A** Sox2 gene and protein expressions were higher in HCP compared to control group at E105. However, as gestation progressed, its expression notably decreased. **B** Upregulation of Vimentin and Aq4 relative expressions were seen, particularly after E125. Western blot analysis showed significantly higher Vimentin protein level in the hydrocephalic groups at E140. **C** MOBP and MOG relative expressions upregulated at E105 but after E125, their gene expressions and MBP protein level decreased significantly (Data in the bar graphs represent mean ± SEM, green bars: control, blue bars: HCP) (*$p < 0.05$, **$p < 0.01$). **D** Immunostainings of Sox2 (green), Vimentin (red), MBP (magenta) and DAPI in control and hydrocephalic brains at E105, E125 and E140 (×20, scale bar 50 µm)

being suppressed by Pax6 [33]. Besides that, DCX serves as a marker for migrating neuroblasts and immature neurons, which is crucial for neuronal differentiation and migration [36, 39], overall shaping the complex processes underlying cortical development and neuronal subtype specification.

We observed dysregulation in the expression of Ascl1 and Tbr2 genes during different stages of pregnancy in hydrocephalic samples compared to controls, suggesting disturbances in cortical neuron differentiation pathways. Our study demonstrated initial increases in the expression of the intermediate progenitor cell markers Ascl1 and Tbr2 at E105, followed by divergent trends in subsequent stages (E125 and E140). Throughout these periods, Ascl1 gene expression decreased, while Tbr2 gene expression significantly increased in hydrocephalic samples compared to those in the control group ($p < 0.001$, $p < 0.001$ and $p < 0.001$, control and HCP E105, E125 and E140, respectively). Furthermore, we found that both the gene expression and protein levels of DCX increased significantly in hydrocephalic fetuses at E105 ($p = 0.001$ and $p = 0.001$, control and HCP E105, respectively), with subsequent downregulation at term ($p = 0.004$ and $p = 0.001$, control and HCP E140, respectively) (Fig. 4A).

To determine the distribution of immature neurons and characterize the cells forming PH in hydrocephalic samples at term, we stained the cells with DCX. It was observed that PHs consisted of densely packed, round shaped, irregularly stained DCX-positive cells with strong basophilic nuclei and a thin cytoplasmic rim, located beneath denuded areas (Fig. 4B).

Astroglial reaction occurring in denuded ventricular areas becomes more severe as pregnancy progresses

In the case of HCP, these denuded areas trigger a periventricular astroglial reaction, featuring hypertrophy and hyperplasia of astrocytes and forming a new layer mimicking ependymal cells to maintain homeostasis [40–43].

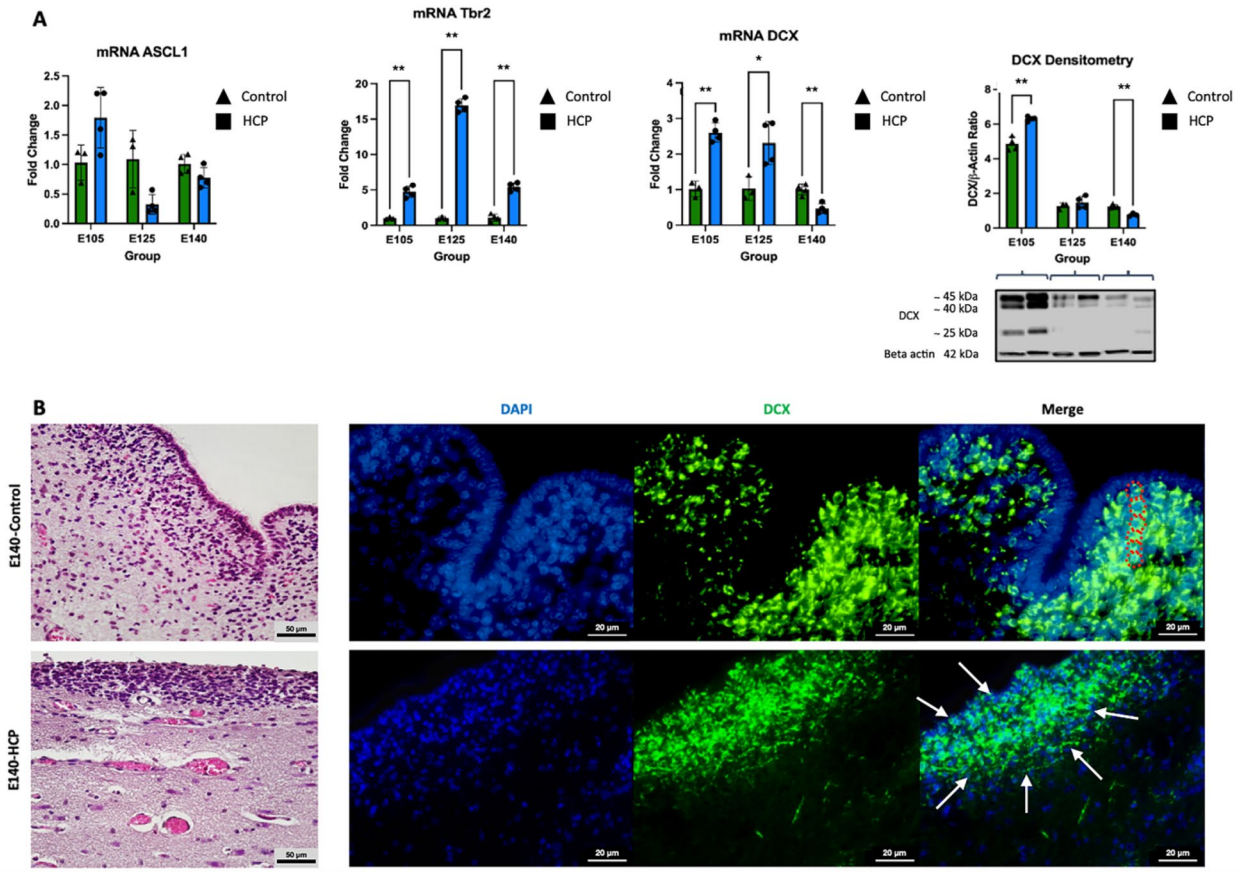

Fig. 4 Alterations in the expression of Ascl1, Tbr2 and DCX during different stages of pregnancy in HCP. **A** The relative expression of Ascl1 and Tbr2 initially increased, followed by opposite trends at E125 and E140. Throughout these periods, Ascl1 expression decreased, whereas Tbr2 expression upregulated in HCP. Besides that, DCX showed significant increases in both gene expression and protein levels in hydrocephalic fetuses at E105, but then downregulation was seen at E140 (Data in the bar graphs represent mean ± SEM, green bars: control, blue bars: HCP) (*$p < 0.05$, **$p < 0.01$). **B** In normal brain tissue, DCX-positive cells in the SVZ are arranged in chains (red dashed circles), whereas in hydrocephalic samples, PHs have densely packed, disorganized DCX-positive cells (white arrows indicate the borders of the cell cluster) (H&E: × 20, scale bar 50 µm, IF: × 40, scale bar 20 µm)

Reactive astrocytes in HCP exhibit increased expression of intermediate filament proteins such as GFAP and vimentin, which are crucial for organizing cytoplasmic structures [28, 40]. Additionally, Aquaporin 4 (Aq4), predominantly found in periventricular areas, is overexpressed in reactive astrocytes in hydrocephalic brains as well and facilitates water entry to restore osmotic equilibrium [44].

Since the astrocytic markers, GFAP and vimentin, are also expressed in RGCs, we sought to evaluate astroglial reactivity in the VZ and SVZ in HCP fetuses by also assessing Aq4 gene expression, at each time point. From early stages in HCP, significant increases in GFAP, Vimentin, and Aq4 gene expression were seen, with a more pronounced increase in the later stages of pregnancy (E140) ($p < 0.001$, $p < 0.001$ and $p < 0.001$, control and HCP E140, respectively). Western blot analysis further confirmed significantly higher protein levels of GFAP and Vimentin, particularly at term, in the hydrocephalic groups, suggesting an intensified astroglial response as HCP progresses ($p = 0.048$ and $p = 0.025$, control and HCP E140, respectively) (Fig. 2B, 3B).

In these regions, the proliferation of reactive astrocytes follows a distinct pattern. Initially, they are arranged loosely and express vimentin and GFAP. In later stages, some of these astrocytes form small clusters of cells, which then become a highly compact, continuous layer [42]. In our study, immunofluorescence staining revealed differences in GFAP and vimentin staining patterns between control and HCP samples. While GFAP and vimentin were predominantly expressed in NPCs within the VZ of control groups, hydrocephalic samples, especially at E140, exhibited more prominent staining of reactive astrocytes in the SVZ under the denuded areas. Additionally, vimentin showed a more chaotic and punctate staining pattern in hydrocephalic samples, suggesting

altered astroglial morphology and organization (Fig. 2D, 3D). Interestingly, at E105, GFAP + astrocytes found in the VZ of hydrocephalic brains also expressed Pax6 (Fig. 2E). These findings demonstrate that Pax6- and GFAP-positive cells in the VZ exposed to CSF identified early in development suggesting that NPC Pax6 cells may undergo differentiation into astrocytes and lead to astrogenesis, potentially contributing to the maintenance of homeostasis and facilitating repair processes.

Early onset-fetal hydrocephalus reduces the formation of myelin

During brain development, gliogenesis follows neurogenesis and produces astrocytes and oligodendrocytes [45]. Oligodendrocytes, crucial for myelin formation in the central nervous system, undergo different developmental stages from oligodendrocyte progenitor cells (OPCs) to mature myelinating oligodendrocytes (OLs). HCP also leads to white matter damage as the enlargement of the ventricles stretches and compresses the surrounding white matter, potentially compromising myelin, axons, and blood vessels [15].

Transcription factors involved in gliogenesis are not restricted to astrocyte differentiation; they also play crucial roles in oligodendrocyte production [40]. To investigate the involvement of transcriptional regulators of oligodendrocyte differentiation, oligodendrocyte transcription factor 2 (Olig2) and Sox10 were used as OPC markers, while myelin basic protein (MBP), myelin-associated oligodendrocyte basic protein (MOBP), and myelin oligodendrocyte glycoprotein [46] were used as markers for OLs [47, 48]. Olig2 serves as a master regulator of the early stages of oligodendrocyte development [48, 49], acting as an upstream regulator of Sox10 [50]. Our findings demonstrated an upregulation in the gene expression of MOBP and MOG in the HCP group compared to that in the control group at gestational day E105 ($p < 0.001$and $p = 0.049$, control and HCP E105, respectively), followed by a notable decrease in Sox10, MOBP, and MOG gene expression during the mid and late stages of pregnancy ($p = 0.002$ and $p = 0.009$, $p = 0.02$ and $p = 0.02$, $p > 0.05$ and $p = 0.049$ control and HCP E125 and E140, respectively). MBP protein expression was not detected in the early stage (E105), as myelin formation had not yet occurred. However, both MBP and Olig2 protein expressions showed a significant downregulation in the HCP groups, in later stages (E125 and E140) ($p = 0.029$ and $p = 0.02$, $p = 0.01$ and $p = 0.01$, control and HCP E125 and E140, respectively) (Figs. 2C, 3C).

Immunofluorescence staining, it was observed that, particularly at E125, Pax6-positive NPCs translocated to the CSF were also positive for Olig2, indicating that NPCs migrating to the CSF could potentially represent a subset progressing towards an oligodendrocyte fate during development (Fig. 5A, B). The downregulation of Sox10 mRNA and the translocation of Pax6 + Olig2 + cells into the CSF observed in HCP at E125 may correlate with a decrease in Olig2 protein level at later stage (E140) compared to control.

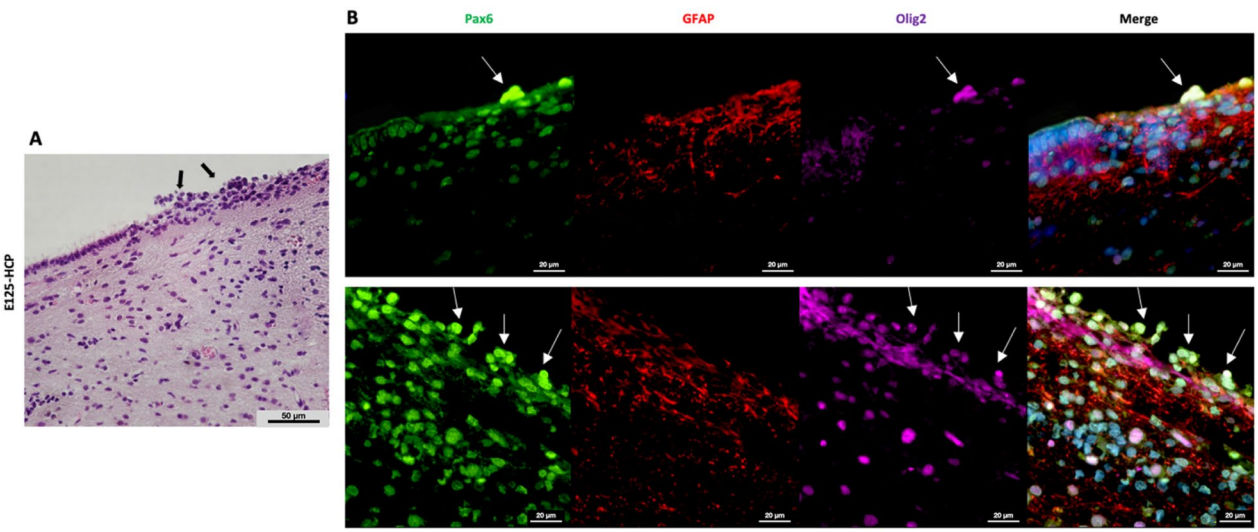

Fig. 5 **A** In the denuded area, neural precursors have been reaching the ventricular lumen (black arrows) (E125-HCP, × 20, scale bar 50 µm), **B** In these areas where astrocytosis (GFAP, red) was also seen, these cells were co-stained with Pax6 (green) and Olig2 (magenta) (white arrows) (× 40, scale bar 20 µm)

Discussion

The complex and close relationship between fetal-onset HCP and abnormal neurogenesis has been further elucidated by studies emphasizing the common pathology of the VZ affecting NSCs and then multiciliate ependymal cells [5, 10, 17]. Insights from the intracisternal BioGlue-induced fetal lamb obstructive HCP model enhance our understanding of how this disruption in VZ contributes to disturbances in both neurogenesis and gliogenesis, providing the first detailed description of neuropathology in this model, and further studies on this topic is expected.

Before discussing the findings of the study, we found it appropriate to compare the HCP model induced by Bioglue that we used in this study with HCP models created with non-invasive methods. Comparing the BioGlue-induced HCP model to non-invasive congenital HCP models such as maternal treatment with teratogens, exposure to viruses, radiation, mineral or vitamin deficient diets, and genetic mutations (the hydrocephalus Texas (HTx) rat or the hyh mice) highlights differences in methodologies, mechanisms, and.

insights into the disease's pathophysiology and potential treatments. The BioGlue-induced hydrocephalus model is created in large animals such as lambs, contrasts with non-invasive congenital hydrocephalus models that often use small animals like mice and rats. The use of large animals offers advantages, especially since it is applied to gyrencephalic brains, which are anatomically and physiologically more similar to the human brain and where pathology is observed throughout the brain, making surgical techniques and their outcomes more directly translatable to clinical settings [51], whereas the mouse and rat brains frequently used in other fetal hydrocephalus models mentioned above are lissencephalic. These fetal HCP models are effective for examining the natural progression of the malformation during the fetal period and facilitates detailed studies on genetic pathways and various pharmacological agents but any intrauterine application of shunt systems and devices is often challenging [1, 52]. While they are less expensive and easier to maintain, they may not fully reflect the complexity of human neuroanatomical structures. Thus, each model has unique strengths and limitations, making them complementary depending on the research focus—whether it is surgical intervention applicability or genetic and developmental pathway analysis.

Fetal-onset HCP presents challenges due to concurrent pathophysiological mechanisms, including increased intraventricular pressure, compression and stretching of brain parenchyma, ischemia/hypoxia, and structural alterations of neurons and ependymal cells, causing brain anomalies [15, 42]. Disruption of the VZ in hydrocephalic human fetuses, evident as early as 16 GW, results in distinct consequences depending on the timing and extent of disruption. While perinatal VZ disruption results from ependymal loss and lining disruption/denudation, fetal VZ disruption leads to the loss of NSCs/NPCs [10]. VZ disruption in various brain regions, such as the Sylvian aqueduct [13, 16, 42] and pallium, affects neuro/gliogenesis and can lead to specific structural abnormalities such as PHs [53], contributing to neurological deficits observed in hydrocephalic children, that are not resolved by CSF shunting.

Studies in animal models such as hyh mice [54] and kaolin-induced HCP in rats [55] and ferrets [56] show that disruption of VZ integrity leads to an initial and progressive surge in NSC proliferation to generate new neurons to replace damaged ones. This is followed by a gradual decline until they disappear entirely and impairing neuronal repair, suggesting that NSCs play a role in both the pathophysiology and repair process of HCP. However, this mechanism has a limit where NSC proliferation is not matched by apoptosis, leading to a reduction in NSCs, as seen in acute brain injuries [57]. Furthermore, loss of radial glia/NSCs that form the VZ [9] and increased cell death due to cerebral ischemia [24, 58–60] contribute to the reduced numbers of SVZ progenitors, potentially affecting neurogenesis. A recent study found a significant decrease in proliferative cells in the subventricular zone of hydrocephalus-induced pigs and this reduction in SVZ area was significantly associated with an increase in ventricular volume [20].

Pax6 is a central regulator, that facilitates the transition from NECs to apical radial glia (aRGs) [30], and also influences the differentiation of specialized neuronal subtypes, including glutamatergic and dopaminergic neurons [61]. Another key transcription factor, Sox2 (SRY -sex determining region Y- box 2), cooperates with Pax6 in gene regulation [31] and is essential for maintaining the proliferation and differentiation of NSCs throughout neurogenesis [36]. Thus, the temporal and spatial expression patterns of these factors regulate the sequential generation of cortical neurons, from early progenitors to postmitotic neurons, ensuring the proper formation of cortical layers and the establishment of neuronal diversity. Based on the literature, our results indicate a potential association between disruption in VZ and alterations in Pax6 and Sox2 expression observed in hydrocephalic samples. Although the initial surge in NSC/NPC proliferation observed in early-stage HCP (E105) fetal lambs may represent a compensatory mechanism aimed at generating new neurons to replace damaged ones, the subsequent decline in Pax6 and Sox2 expression, particularly Sox2 expression at term, suggests a failure in neurogenic

processes and impaired neuronal repair, aligning with the pathophysiology of HCP observed in animal models [57].

Next, we focused on comprehending the modifications in transcription factors that determine the fate of neuronal differentiation in HCP. The consequences of VZ disruption extend to the differentiation of two main populations of cortical neurons, GABAergic and glutamatergic, with disruptions of different anatomical origins. In mice, disruption of the VZ in the ganglionic eminences impairs the neurogenesis of GABAergic neurons [16, 53], while disruption of the pallium primarily affects glutamatergic neurons and gliogenesis [9]. This disruption leads to a shift in the balance of neuron production, resulting in early overproduction of neurons in the absence of a VZ, followed by progressive loss of progenitor cells. Furthermore, it has also been shown that Pax6 overexpression accelerates neural maturation towards early neuronal precursors without ultimately affecting net neurogenesis, instead leading to a decline in NPCs over time [62]. These insights indicate the critical role of VZ integrity in organizing proper cortical development and the complex relationship between VZ disruption, neurogenesis, and the pathogenesis of HCP [63–65].

Our research revealed alterations in the expression of Ascl1 and Tbr2 genes during different gestational stages in hydrocephalic samples compared to controls, indicating disruptions in cortical neuronal differentiation pathways, characterized by initial increases in Ascl1 and Tbr2 expression at E105, followed by distinct trends in subsequent stages, along with significant upregulation of DCX gene expression and protein levels at E105, followed by downregulation at term. Our findings corroborate the observations in the literature, indicating a shift in the balance of neuron production in HCP, characterized by an early overproduction of neurons followed by a progressive loss of progenitor cells and neuroblasts. In addition, our data showed that as neurogenesis progressed after E125, Pax6 and Sox2 levels decreased while Ascl1 levels increased. This finding suggested that a subset of genes involved in neurogenesis, regulated by Pax6 and Sox2 in NPCs, may also be targeted by other transcription factors such as Ascl1 [31].

Interestingly, we demonstrated that the transcription factors Ascl1 and Tbr2 act oppositely in intermediate progenitor cells. These transcription factors are known to serve distinct functions. While Ascl1 alone directs cells towards a GABAergic inhibitory interneuron fate in the ventral telencephalon [66, 67], its collaboration with dopaminergic, cholinergic, or serotonergic factors induces the formation of dopaminergic, cholinergic, or serotonergic neuronal subtypes, respectively. On the other hand, Tbr2 is crucial for specifying glutamatergic neurons within the cerebral cortex and is involved in regulating the organization of excitatory neuron circuits and promoting neurogenesis [37]. Therefore, our data suggest that various types of neurons and cortical regions may be impacted differently in HCP. Nonetheless, further studies are warranted to validate these findings. Overall, our research contributes to understanding the complex interplay between VZ disruption and the role of key transcription factors in neurogenesis in HCP.

RGCs play a central role during early brain development and provide neural and glial precursors. After neurogenesis, RGCs undergo a gliogenic switch that leads to the differentiation of astrocyte precursors, first into intermediate progenitor cells and then into mature astrocytes [68]. Astrogenesis relies on the inhibition of neurogenic genes. Following commitment to the astrocyte lineage, progenitors migrate along radial glial cell processes, ultimately populating the entire central nervous system and expressing markers such as GFAP, vimentin, S100β, Aldh1L1, glutamine synthase and Aq4 [40]. Reactive astrogliosis, a response to pathological conditions, requires morphological changes to protect the central nervous system from inflammation and neurodegeneration. This astroglial reaction may also diminish the proliferative activity of neural progenitors, as observed in adult rabbits with silicone oil-induced HCP [69]. Unlike microglia, astrocytes undergo slower morphological changes, with hypertrophy and GFAP upregulation occurring within 2–3 days after injury [40]. These activated astrocytes release cytokines that recruit other astrocytes, resulting in scar formation, and potentially interrupting neuronal regeneration [70]. And even in cases of successful shunting, glial scars persist in hydrocephalic brains [22]. Additionally, it has also been shown that these astrocytes contribute to ependymal repair by acquiring ependymal cell-like properties in hyh mice [42, 44, 71].

Studies in H-Tx rats have demonstrated a progressive rise in GFAP RNA levels with the advancement of HCP, indicating the role of GFAP in reactive astrogliosis [19, 72]. Besides GFAP, the upregulation of vimentin, which is typically found in early astrocyte development [73], and the overexpression of Aq4 in periventricular astrocytes [44] are also observed in reactive astrocytes in HCP. Current research displayed notable increases in the gene and protein expression of GFAP, Vimentin, and Aq4, with a more prominent rise observed later in pregnancy (E140), suggesting an increased astroglial response throughout HCP progression. Moreover, in hydrocephalic animals, overexpression of Pax6 in early gestational stage (E105) and its co-expression with GFAP + cells within the VZ exposed to CSF, suggest that these cells may be committed to astrocytic differentiation, potentially counteracting neurogenesis as shown previously in spina bifida [74]. Overall, these findings highlight the dynamic response

of astrocytes to HCP for maintaining brain homeostasis under pathological conditions.

Previous studies have reported that periventricular axons are the primary targets involved in hydrocephalic brain damage. Investigations have shown that direct damage to oligodendrocytes by HCP causes impaired myelin production in immature hydrocephalic rats [75], increases oligodendrocyte cell death in periventricular white matter of the juvenile hydrocephalic pigs [20], and disrupts differentiation and migration of oligodendrocyte progenitors, leading to reduced myelin production [76]. Therefore, HCP may inhibit myelin formation in the brain by a variety of concurrent factors, such as stretching and compression, edema, hypoxia, and oligodendrocyte death [1]. Our results revealed an initial upregulation of MOBP and MOG gene expression in the HCP group at E105, followed by a subsequent decrease in Sox10, MOBP, and MOG gene expression during pregnancy, and both MBP and Olig2 protein expression declined significantly in the HCP groups at later stages (E125 and E140), representing myelin damage which was also evident in immunostaining. Additionally, Olig2 is a critical patterning factor in neurogenesis as well as oligodendrogenesis, and its downregulation results in an increased astrocytic lineage [62, 77]. Hence, this might also contribute to the pronounced periventricular astroglial reaction. Therefore, disarrangement of transcription factors such as Olig2 and Pax6, coupled with the overexpression of astrocytic markers, could serve as a reasonable mechanism triggering the early differentiation of NPCs into astrocytes. We consider this to be a protective response following injury in denuded areas.

Finally, we attempted to estimate the optimal timing for fetal intervention in HCP. The focus of most studies has been on the postnatal effects of elevated intracranial pressure and the effectiveness of standard CSF diversion procedures (ventricular shunting or neuroendoscopic procedures). However, the timing of these interventions is often inadequate or late, and the fetal-onset HCP leads to a range of neurological deficits [78]. During neuronal development, the peak of neural proliferation and migration in humans occurs between the 12th and 18th GW, followed by a gradual decline. Gliogenesis follows neurogenesis and continues postnatally, while ependymogenesis initiates around the 18th GW and is completed after birth [10]. Disruption of the VZ in hydrocephalic human fetuses begins in the second trimester and extends into the third trimester, coinciding with the timing of HCP diagnosis by ultrasound [10]. In addition, it is well-known that fetal surgery for myelomeningocele is commonly performed between the 19th and 25th GW, and there is often a high incidence of concomitant VZ disruption and HCP [10]. In this BioGlue-induced fetal hydrocephalic lamb model, we observed VZ disruption as early as E105, the earliest stage we examined. Subsequently, we demonstrated a decrease in NPCs, an increase in astroglial activity, and the onset of myelin damage, particularly after E125. Considering all the information mentioned above and based on the literature, it was found that performing surgical intervention between E105 and E125, which corresponds to the end of the second trimester and the beginning of the third trimester in humans, indicating an appropriate and effective therapeutic window for prenatal surgery before irreversible processes begin **(**Fig. 6**).**

In recent years, endoscopic third ventriculostomy (ETV) has gained popularity and has begun to be used even in younger patients and it appears to be particularly effective for certain conditions such as aqueductal stenosis [79]. Moreover, a prenatal surgical approach demonstrated in a fetal sheep model, suggested that performing ETV prenatally is feasible and could effectively reduce ventricle pressure, dilatation, brain mantle compression, and prevent permanent damage during brain development. This prenatal approach could offer an alternative and promising treatment option for congenital obstructive HCP cases without genetic anomalies compared to postnatal shunting [52, 80].

Although there have been considerable advancements in fetal diagnosis, progress in the prenatal treatment of congenital HCP remains insufficient and evolving. While derivative surgery aims to reduce brain damage, it is not a cure for HCP-induced brain maldevelopment [9]. It can prevent some pathological changes [81], but functional improvements still remain incomplete [15], with persistent ependymal denudation, impaired capillary circulation [76] and incomplete restoration of neurons and myelin formation [15, 75, 82, 83].

Recent studies emphasize the evolution of HCP research from traditional surgical methods to innovative therapies that target the disease's biological mechanisms. The NIH workshop in 2007 identified the need for exploring novel medical devices and the potential of stem cell therapy for neuroregeneration as key future research directions [14]. Despite the limited success of non-surgical approaches over decades, recent advances have shown promising results from pharmacological approaches like minocycline [1, 84, 85] and erythropoietin [86], which are specifically neuroprotective. Besides these, targeted pharmacological agents such as mTOR inhibitor rapamycin [87] and anti-inflammatory drug Bindarit [88] have been effective in preventing ventriculomegaly and improving neurological functions in animal models. These developments suggest a shift towards treating HCP as a manageable neurodevelopmental condition rather than just a surgical challenge. Innovative methods like delivery of neurospheres into

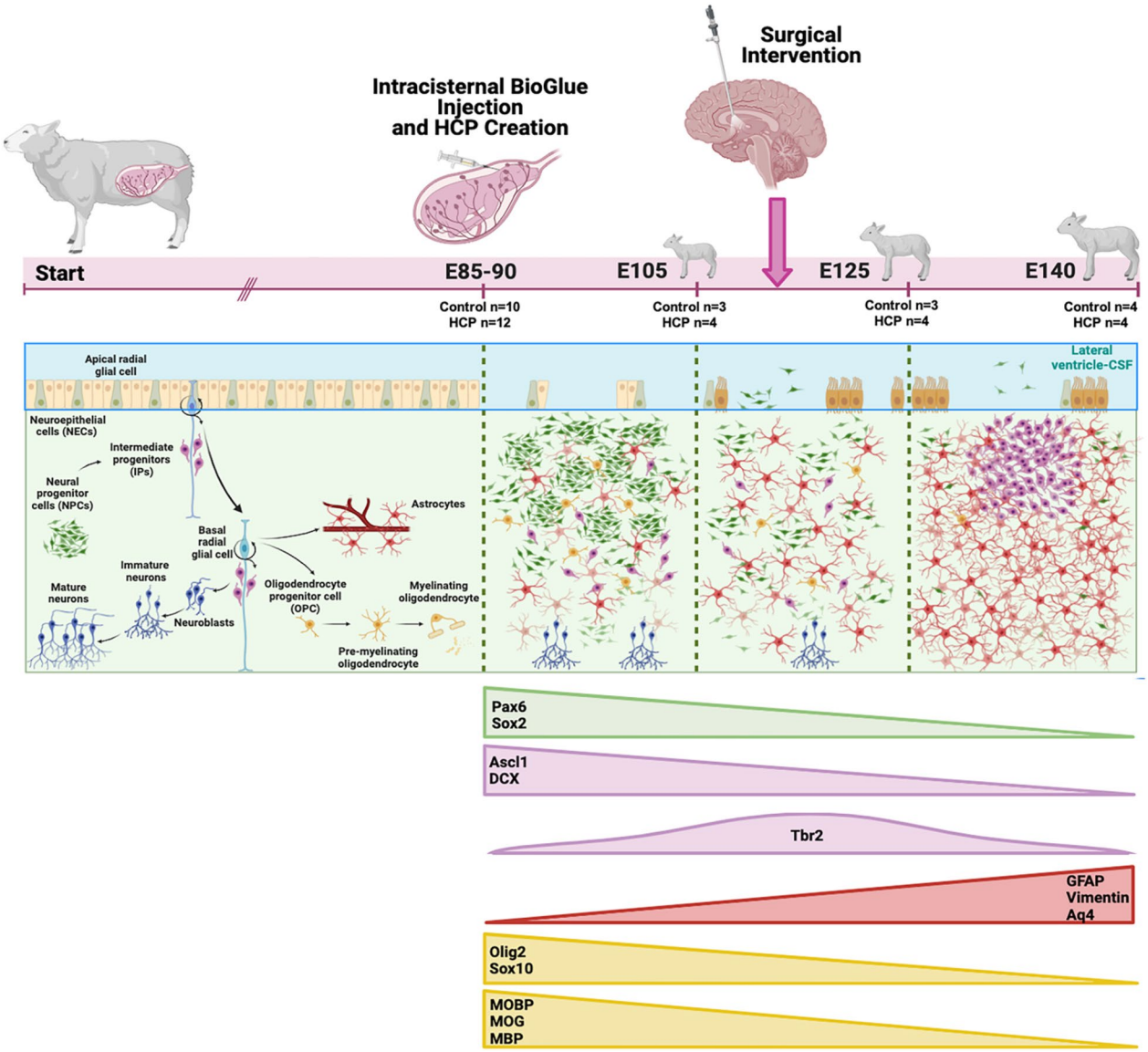

Fig. 6 Alterations in neurogenesis and gliogenesis in fetal-onset hydrocephalus. During normal early neurodevelopment, neuroepithelial cells (NECs) in the neural tube differentiate into multipotent apical radial glial cells (aRGs) in the VZ. Subsequently, asymmetric divisions of aRGs generate basal progenitors (BPs) in the SVZ, including basal radial glial cells (bRGs) and basal intermediate progenitors (bIPs), which contribute to the production of cortical neurons and macroglia, essential for the development of the neocortex and formation of cortical folds. In this research on hydrocephalus in fetal lambs, disruptions in the VZ were observed as early as E105. Initial compensatory mechanisms occurred through increased proliferation of the NSCs and NPCs, followed by decreases in important neurogenic regulators such as Pax6 and Sox2, particularly at term. Notably, this surge was associated with significant upregulation of DCX, suggesting active neurogenesis at this early stage. However, this proliferation was accompanied by a decline in the expression of critical neurogenic markers such as Pax6 and Sox2, particularly noticeable towards the term, indicating compromised neuronal repair capabilities. Additionally, alterations in the expression of Ascl1 and Tbr2 pointed to disrupted neuronal differentiation pathways, with fluctuating expression patterns evident across various gestational stages. The progression of hydrocephalus was also marked by increased expression of astroglial markers (GFAP, Vimentin, and Aq4), along with pronounced myelin damage indicated by the reduced expressions of MOBP, MOG, and Sox10 as the gestation advanced. Collectively, these findings suggest that surgical intervention between E105 and E125 may offer a critical therapeutic window, providing a potentially effective period for prenatal surgery to mitigate the irreversible damage due to hydrocephalus (created on BioRender.com)

the CSF, have demonstrated potential to mitigate neurological impairments in HCP [10]. Additionally, preliminary experiments with stem cell grafting indicated that these transplanted cells can repair disrupted ventricular zones and correct abnormalities in neurogenesis, offering hope not only for treating HCP but also for potentially

addressing other neurodevelopmental disorders through regenerative and pharmacological therapies [10, 11, 89, 90]. This research could also led to discover tailored pharmacological interventions, such as growth factors and hormones, which influence the differentiation of neurons and glia, thus facilitating the development of novel medications to regulate the normal development of cerebral cortex (5).

Certain study limitations do exist. First, the use of BioGlue-induced hydrocephalus model in fetal lambs may not entirely mimic the complex neurodevelopmental processes and naturally occurring pathophysiological mechanisms of the disease in humans due to species differences, which could affect the translatability of the findings. Secondly, in our BioGlue-induced hydrocephalus model, ventriculomegaly was induced predominantly symmetrically across samples due to its application within the cisterna magna that cause aqueductal stenosis. However, individual variations in response could lead to asymmetric ventriculomegaly that could introduce additional complexities. This could introduce variations in the histological and molecular data, potentially affecting the interpretation of our results. Another limitation is the sample size, which, although sufficient for analyses, might be small for detecting more subtle changes and variations within and between groups. Lastly, the study focuses primarily on the immediate impacts of hydrocephalus on neurogenesis and gliogenesis without long-term follow-up to assess the overall survival and neurological outcomes.

A better understanding of pathophysiological mechanisms involved in fetal-onset HCP and emerging developments in fetal surgical interventions presenting promising opportunities for early interventions to address dysregulation in neuro/gliogenesis in HCP.

Conclusion

Hydrocephalus is a prevalent condition in routine neurosurgery, representing one of the most frequent congenital anomalies and a leading cause of neurosurgical procedures in pediatric patients. Today, while surgical intervention is feasible postnatally, numerous irreversible alterations have typically already occurred during fetal development and irreversible by the time the surgery is currently performed. The present investigation identified alterations in neuro-/gliogenesis associated with fetal-onset HCP throughout pregnancy and predicted the ideal timing for a potential prenatal surgical intervention. Prenatal surgery for obstructive isolated HCP could become a therapeutic option that may improve patient outcomes in the future.

Abbreviations

Aq4	Aquaporin 4
aRGs	Apical radial glias
bIPs	Basal intermediate progenitors
BPs	Basal progenitors
bRGs	Basal radial glial cells
BSA	Bovine serum albumin
cDNA	Complementary DNA
CP	Cortical plate
CSF	Cerebrospinal fluid
DCX	Doublecortin
ETV	Endoscopic third ventriculostomy
GD	Gestational day
GFAP	Glial fibrillary acidic protein
GW	Gestational week
H&E	Hematoxylin and eosin
HCP	Hydrocephalus
MAP	Microtubule-associated protein
MBP	Myelin basic protein
MOBP	Myelin-associated oligodendrocyte basic protein
MOG	Myelin oligodendrocyte glycoprotein
NECs	Neuroepithelial cells
NPCs	Neural progenitor cells
NSCs	Neural stem cells
OLs	Oligodendrocytes
OPCs	Oligodendrocyte progenitor cells
PBS	Phosphate-buffered saline
PH	Periventricular heterotopia
RGCs	Radial glial cells
RT	Room temperature
Sox2	SRY (sex determining region Y) box 2
SVZ	Subventricular zone
Tbr2	T-box brain gene 2
VZ	Ventricular zone

Supplementary Information

The online version contains supplementary material available at https://doi.org/10.1186/s12987-025-00630-3.

Additional file 1: Tables of detailed statistical analyses for each marker used in this study. It presents mean values and results of statistical tests, including the two-sample t-tests for comparisons between control and hydrocephalus-induced groups. Each table is labeled to correspond with the specific marker it discusses

Acknowledgements

We would like to acknowledge the contributions of all those who have supported this work.

Author contributions

Conception and design: DK, MO, SD and JLP. Technical/material support: DK, KL, SD, HKO, JLE, FSM, LP, MO, JLP. Funding: JLE, FSM, MO and JLP. Acquisition of data: DK and MO. Analysis and interpretation of data: DK and MO. Drafting the article: DK and MO. Critically revising the article: DK, SD, HKO, FSM, MO and JLP. Statistical analysis: MO. Study supervision: MO and JLP. All authors contributed to the article and approved the final manuscript.

Funding

This work was supported by Prof. Jose L. Peiro internal CCHMC Pediatric Surgery Division funding, the Rudi Schulte Research Institute (RSRI) (USA), and by the Instituto Carlos III (ISCIII) through the project " PI21/01886" and co-funded by the European Union. Dicle Karakaya was supported with a research scholarship by The Scientific and Technological Research Council of Turkey (TUBITAK) (2021/1/2219/1059B192100803) (Turkey).

Availability of data and materials

The datasets used and/or analysed during the current study are available from the corresponding author on reasonable request.

Declarations

Ethics approval and consent to participate

The experimental procedures involving animals were performed according to the National Institutes of Health Guidelines for Care and Use of Laboratory Animals and were approved by the Institutional Animal Care and Use Committee at Cincinnati Children's Hospital Medical Center (IACUC 2021–0008), and also approved by the Institutional Animal Care and Use Committee (IACUC: ES100370001499) at the Jesus Uson Minimally Invasive Surgery Centre, Caceres, Spain.

Consent for publication

Not applicable.

Competing interests

The authors declare no competing interests.

Author details

[1]The Center for Fetal and Placental Research, Cincinnati Children'S Hospital Medical Center (CCHMC), 3333 Burnet Avenue, MLC 11025, T8.605, Cincinnati, OH 45229-3039, USA. [2]Department of Neurosurgery, Hacettepe University, Ankara, Turkey. [3]Pediatric Surgery Division, Hospital Universitario La Paz, Madrid, Spain. [4]Centro de Cirurgia de Minima Invasion Jesus Uson (CCMIJU), Caceres, Spain. [5]Department of Radiation Oncology, College of Medicine, University of Cincinnati, Cincinnati, OH, USA. [6]University of Cincinnati Cancer Center (UCCC), Cincinnati, OH, USA. [7]University of Cincinnati Brain Tumor Center (BTC), Cincinnati, OH, USA. [8]Department of Surgery, College of Medicine, University of Cincinnati, Cincinnati, OH, USA.

Received: 13 July 2024 Accepted: 10 February 2025
Published online: 24 February 2025

References

1. McAllister JP 2nd. Pathophysiology of congenital and neonatal hydrocephalus. Semin Fetal Neonatal Med. 2012;17(5):285–94.
2. Kulkarni AV, Shams I. Quality of life in children with hydrocephalus: results from the Hospital for Sick Children. Toronto J Neurosurg. 2007;107(5 Suppl):358–64.
3. Del Bigio MR. Neuropathology and structural changes in hydrocephalus. Dev Disabil Res Rev. 2010;16(1):16–22.
4. Jones HC, Klinge PM. Hydrocephalus 2008, 17–20th September, Hannover Germany: a conference report. Cerebrospinal Fluid Res. 2008;5:19.
5. Guerra M. Neural stem cells: are they the hope of a better life for patients with fetal-onset hydrocephalus? Fluids Barriers CNS. 2014;11:7.
6. Guerra M, Blazquez JL, Rodriguez EM. Blood-brain barrier and foetal-onset hydrocephalus, with a view on potential novel treatments beyond managing CSF flow. Fluids Barriers CNS. 2017;14(1):19.
7. Schiff SJ, Kulkarni AV, Mbabazi-Kabachelor E, Mugamba J, Ssenyonga P, Donnelly R, et al. Brain growth after surgical treatment for infant postinfectious hydrocephalus in Sub-Saharan Africa: 2-year results of a randomized trial. J Neurosurg Pediatr. 2021;28(3):326–34.
8. Lindquist B, Carlsson G, Persson EK, Uvebrant P. Learning disabilities in a population-based group of children with hydrocephalus. Acta Paediatr. 2005;94(7):878–83.
9. Rodriguez EM, Guerra MM, Vio K, Gonzalez C, Ortloff A, Batiz LF, et al. A cell junction pathology of neural stem cells leads to abnormal neurogenesis and hydrocephalus. Biol Res. 2012;45(3):231–42.
10. Rodriguez EM, Guerra MM. Neural stem cells and fetal-onset hydrocephalus. Pediatr Neurosurg. 2017;52(6):446–61.
11. Duy PQ, Rakic P, Alper SL, Robert SM, Kundishora AJ, Butler WE, et al. A neural stem cell paradigm of pediatric hydrocephalus. Cereb Cortex. 2023;33(8):4262–79.
12. Sival DA, Guerra M, den Dunnen WF, Batiz LF, Alvial G, Castaneyra-Perdomo A, et al. Neuroependymal denudation is in progress in full-term human foetal spina bifida aperta. Brain Pathol. 2011;21(2):163–79.
13. Wagner C, Batiz LF, Rodriguez S, Jimenez AJ, Paez P, Tome M, et al. Cellular mechanisms involved in the stenosis and obliteration of the cerebral aqueduct of hyh mutant mice developing congenital hydrocephalus. J Neuropathol Exp Neurol. 2003;62(10):1019–40.
14. Williams MA, McAllister JP, Walker ML, Kranz DA, Bergsneider M, Del Bigio MR, et al. Priorities for hydrocephalus research: report from a National Institutes of Health-sponsored workshop. J Neurosurg. 2007;107(5 Suppl):345–57.
15. Del Bigio MR. Pathophysiologic consequences of hydrocephalus. Neurosurg Clin N Am. 2001;12(4):639–49.
16. Jimenez AJ, Tome M, Paez P, Wagner C, Rodriguez S, Fernandez-Llebrez P, et al. A programmed ependymal denudation precedes congenital hydrocephalus in the hyh mutant mouse. J Neuropathol Exp Neurol. 2001;60(11):1105–19.
17. Guerra MM, Henzi R, Ortloff A, Lichtin N, Vio K, Jimenez AJ, et al. Cell junction pathology of neural stem cells is associated with ventricular zone disruption, hydrocephalus, and abnormal neurogenesis. J Neuropathol Exp Neurol. 2015;74(7):653–71.
18. Karimy JK, Reeves BC, Damisah E, Duy PQ, Antwi P, David W, et al. Inflammation in acquired hydrocephalus: pathogenic mechanisms and therapeutic targets. Nat Rev Neurol. 2020;16(5):285–96.
19. Miller JM, McAllister JP 2nd. Reduction of astrogliosis and microgliosis by cerebrospinal fluid shunting in experimental hydrocephalus. Cerebrospinal Fluid Res. 2007;4:5.
20. Garcia-Bonilla M, Castaneyra-Ruiz L, Zwick S, Talcott M, Otun A, Isaacs AM, et al. Acquired hydrocephalus is associated with neuroinflammation, progenitor loss, and cellular changes in the subventricular zone and periventricular white matter. Fluids Barriers CNS. 2022;19(1):17.
21. Takano T, Rutka JT, Becker LE. Overexpression of nestin and vimentin in ependymal cells in hydrocephalus. Acta Neuropathol. 1996;92(1):90–7.
22. Mangano FT, McAllister JP 2nd, Jones HC, Johnson MJ, Kriebel RM. The microglial response to progressive hydrocephalus in a model of inherited aqueductal stenosis. Neurol Res. 1998;20(8):697–704.
23. Miyan JA, Khan MI, Kawarada Y, Sugiyama T, Bannister CM. Cell death in the brain of the HTx rat. Eur J Pediatr Surg. 1998;8(Suppl 1):43–8.
24. Del Bigio MR, Zhang YW. Cell death, axonal damage, and cell birth in the immature rat brain following induction of hydrocephalus. Exp Neurol. 1998;154(1):157–69.
25. McAllister JP, Guerra MM, Ruiz LC, Jimenez AJ, Dominguez-Pinos D, Sival D, et al. Ventricular zone disruption in human neonates with intraventricular hemorrhage. J Neuropathol Exp Neurol. 2017;76(5):358–75.
26. Oria M, Duru S, Scorletti F, Vuletin F, Encinas JL, Correa-Martin L, et al. Intracisternal BioGlue injection in the fetal lamb: a novel model for creation of obstructive congenital hydrocephalus without additional chemically induced neuroinflammation. J Neurosurg Pediatr. 2019. https://doi.org/10.3171/2019.6.PEDS19141.
27. Duru S, Oria M, Arevalo S, Rodo C, Correa L, Vuletin F, et al. Comparative study of intracisternal kaolin injection techniques to induce congenital hydrocephalus in fetal lamb. Childs Nerv Syst. 2019;35(5):843–9.
28. Wilhelmsson U, Pozo-Rodrigalvarez A, Kalm M, de Pablo Y, Widestrand A, Pekna M, et al. The role of GFAP and vimentin in learning and memory. Biol Chem. 2019;400(9):1147–56.
29. Zhang K, Chen S, Yang Q, Guo S, Chen Q, Liu Z, et al. The oligodendrocyte transcription factor 2 OLIG2 regulates transcriptional repression during myelinogenesis in rodents. Nat Commun. 2022;13(1):1423.
30. Penisson M, Ladewig J, Belvindrah R, Francis F. Genes and mechanisms involved in the generation and amplification of basal radial glial cells. Front Cell Neurosci. 2019;13:381.
31. Thakurela S, Tiwari N, Schick S, Garding A, Ivanek R, Berninger B, et al. Mapping gene regulatory circuitry of Pax6 during neurogenesis. Cell Discov. 2016;2:15045.
32. Ellis P, Fagan BM, Magness ST, Hutton S, Taranova O, Hayashi S, et al. SOX2, a persistent marker for multipotential neural stem cells derived from embryonic stem cells, the embryo or the adult. Dev Neurosci. 2004;26(2–4):148–65.
33. Manuel MN, Mi D, Mason JO, Price DJ. Regulation of cerebral cortical neurogenesis by the Pax6 transcription factor. Front Cell Neurosci. 2015;9:70.
34. Englund C, Fink A, Lau C, Pham D, Daza RA, Bulfone A, et al. Pax6, Tbr2, and Tbr1 are expressed sequentially by radial glia, intermediate progenitor cells, and postmitotic neurons in developing neocortex. J Neurosci. 2005;25(1):247–51.

35. Xing L, Wilsch-Brauninger M, Huttner WB. How neural stem cells contribute to neocortex development. Biochem Soc Trans. 2021;49(5):1997–2006.
36. Zhang J, Jiao J. Molecular biomarkers for embryonic and adult neural stem cell and neurogenesis. Biomed Res Int. 2015;2015: 727542.
37. Sessa A, Ciabatti E, Drechsel D, Massimino L, Colasante G, Giannelli S, et al. The Tbr2 molecular network controls cortical neuronal differentiation through complementary genetic and epigenetic pathways. Cereb Cortex. 2017;27(12):5715.
38. Schuurmans C, Guillemot F. Molecular mechanisms underlying cell fate specification in the developing telencephalon. Curr Opin Neurobiol. 2002;12(1):26–34.
39. Ayanlaja AA, Xiong Y, Gao Y, Ji G, Tang C, Abdikani Abdullah Z, et al. Distinct features of doublecortin as a marker of neuronal migration and its implications in cancer cell mobility. Front Mol Neurosci. 2017;10:199.
40. Schiweck J, Eickholt BJ, Murk K. Important shapeshifter: mechanisms allowing astrocytes to respond to the changing nervous system during development. Injury Dis Front Cell Neurosci. 2018;12:261.
41. Varela MF, Miyabe MM, Oria M. Fetal brain damage in congenital hydrocephalus. Childs Nerv Syst. 2020;36(8):1661–8.
42. Paez P, Batiz LF, Roales-Bujan R, Rodriguez-Perez LM, Rodriguez S, Jimenez AJ, et al. Patterned neuropathologic events occurring in hyh congenital hydrocephalic mutant mice. J Neuropathol Exp Neurol. 2007;66(12):1082–92.
43. Lim DA, Tramontin AD, Trevejo JM, Herrera DG, Garcia-Verdugo JM, Alvarez-Buylla A. Noggin antagonizes BMP signaling to create a niche for adult neurogenesis. Neuron. 2000;28(3):713–26.
44. Roales-Bujan R, Paez P, Guerra M, Rodriguez S, Vio K, Ho-Plagaro A, et al. Astrocytes acquire morphological and functional characteristics of ependymal cells following disruption of ependyma in hydrocephalus. Acta Neuropathol. 2012;124(4):531–46.
45. Miller FD, Gauthier AS. Timing is everything: making neurons versus glia in the developing cortex. Neuron. 2007;54(3):357–69.
46. Almog B, Gamzu R, Achiron R, Fainaru O, Zalel Y. Fetal lateral ventricular width: what should be its upper limit? a prospective cohort study and reanalysis of the current and previous data. J Ultrasound Med. 2003;22(1):39–43.
47. Ye D, Wang Q, Yang Y, Chen B, Zhang F, Wang Z, et al. Identifying genes that affect differentiation of human neural stem cells and myelination of mature oligodendrocytes. Cell Mol Neurobiol. 2023;43(5):2337–58.
48. Wang J, Yang L, Jiang M, Zhao C, Liu X, Berry K, et al. Olig2 ablation in immature oligodendrocytes does not enhance CNS myelination and remyelination. J Neurosci. 2022;42(45):8542–55.
49. Zhou Q, Wang S, Anderson DJ. Identification of a novel family of oligodendrocyte lineage-specific basic helix-loop-helix transcription factors. Neuron. 2000;25(2):331–43.
50. Kuspert M, Hammer A, Bosl MR, Wegner M. Olig2 regulates Sox10 expression in oligodendrocyte precursors through an evolutionary conserved distal enhancer. Nucleic Acids Res. 2011;39(4):1280–93.
51. McAllister JP 2nd, Talcott MR, Isaacs AM, Zwick SH, Garcia-Bonilla M, Castaneyra-Ruiz L, et al. A novel model of acquired hydrocephalus for evaluation of neurosurgical treatments. Fluids Barriers CNS. 2021;18(1):49.
52. Peiro JL, Fabbro MD. Fetal therapy for congenital hydrocephalus-where we came from and where we are going. Childs Nerv Syst. 2020;36(8):1697–712.
53. Ferland RJ, Batiz LF, Neal J, Lian G, Bundock E, Lu J, et al. Disruption of neural progenitors along the ventricular and subventricular zones in periventricular heterotopia. Hum Mol Genet. 2009;18(3):497–516.
54. Jimenez AJ, Garcia-Verdugo JM, Gonzalez CA, Batiz LF, Rodriguez-Perez LM, Paez P, et al. Disruption of the neurogenic niche in the subventricular zone of postnatal hydrocephalic hyh mice. J Neuropathol Exp Neurol. 2009;68(9):1006–20.
55. Khan OH, Enno TL, Del Bigio MR. Brain damage in neonatal rats following kaolin induction of hydrocephalus. Exp Neurol. 2006;200(2):311–20.
56. Di Curzio DL, Buist RJ, Del Bigio MR. Reduced subventricular zone proliferation and white matter damage in juvenile ferrets with kaolin-induced hydrocephalus. Exp Neurol. 2013;248:112–28.
57. Li Y, Wu D, Wu C, Qu Z, Zhao Y, Li W, et al. Changes in neural stem cells in the subventricular zone in a rat model of communicating hydrocephalus. Neurosci Lett. 2014;578:153–8.
58. Mochizuki N, Takagi N, Kurokawa K, Onozato C, Moriyama Y, Tanonaka K, et al. Injection of neural progenitor cells improved learning and memory dysfunction after cerebral ischemia. Exp Neurol. 2008;211(1):194–202.
59. Yeung ST, Myczek K, Kang AP, Chabrier MA, Baglietto-Vargas D, Laferla FM. Impact of hippocampal neuronal ablation on neurogenesis and cognition in the aged brain. Neuroscience. 2014;259:214–22.
60. Chumas PD, Drake JM, Del Bigio MR, Da Silva M, Tuor UI. Anaerobic glycolysis preceding white-matter destruction in experimental neonatal hydrocephalus. J Neurosurg. 1994;80(3):491–501.
61. Sun J, Rockowitz S, Xie Q, Ashery-Padan R, Zheng D, Cvekl A. Identification of in vivo DNA-binding mechanisms of Pax6 and reconstruction of Pax6-dependent gene regulatory networks during forebrain and lens development. Nucleic Acids Res. 2015;43(14):6827–46.
62. Klempin F, Marr RA, Peterson DA. Modification of pax6 and olig2 expression in adult hippocampal neurogenesis selectively induces stem cell fate and alters both neuronal and glial populations. Stem Cells. 2012;30(3):500–9.
63. Takahashi T, Nowakowski RS, Caviness VS Jr. Mode of cell proliferation in the developing mouse neocortex. Proc Natl Acad Sci U S A. 1994;91(1):375–9.
64. Takahashi T, Nowakowski RS, Caviness VS Jr. Early ontogeny of the secondary proliferative population of the embryonic murine cerebral wall. J Neurosci. 1995;15(9):6058–68.
65. Caviness VS Jr, Takahashi T. Proliferative events in the cerebral ventricular zone. Brain Dev. 1995;17(3):159–63.
66. Gohlke JM, Armant O, Parham FM, Smith MV, Zimmer C, Castro DS, et al. Characterization of the proneural gene regulatory network during mouse telencephalon development. BMC Biol. 2008;6:15.
67. Bertrand N, Castro DS, Guillemot F. Proneural genes and the specification of neural cell types. Nat Rev Neurosci. 2002;3(7):517–30.
68. Akdemir ES, Huang AY, Deneen B. Astrocytogenesis: where, when, and how. F1000Res. 2020. https://doi.org/10.12688/f1000research.22405.1.
69. Del Bigio MR, Bruni JE. Periventricular pathology in hydrocephalic rabbits before and after shunting. Acta Neuropathol. 1988;77(2):186–95.
70. Fawcett JW, Asher RA. The glial scar and central nervous system repair. Brain Res Bull. 1999;49(6):377–91.
71. Luo J, Shook BA, Daniels SB, Conover JC. Subventricular zone-mediated ependyma repair in the adult mammalian brain. J Neurosci. 2008;28(14):3804–13.
72. Miller JM, Kumar R, McAllister JP 2nd, Krause GS. Gene expression analysis of the development of congenital hydrocephalus in the H-Tx rat. Brain Res. 2006;1075(1):36–47.
73. Lazic A, Balint V, Stanisavljevic Ninkovic D, Peric M, Stevanovic M. Reactive and senescent astroglial phenotypes as hallmarks of brain pathologies. Int J Mol Sci. 2022. https://doi.org/10.3390/ijms23094995.
74. Oria M, Pathak B, Li Z, Bakri K, Gouwens K, Varela MF, et al. Premature neural progenitor cell differentiation into astrocytes in retinoic acid-induced spina bifida rat model. Front Mol Neurosci. 2022;15: 888351.
75. Del Bigio MR, Kanfer JN, Zhang YW. Myelination delay in the cerebral white matter of immature rats with kaolin-induced hydrocephalus is reversible. J Neuropathol Exp Neurol. 1997;56(9):1053–66.
76. Del Bigio MR. Cellular damage and prevention in childhood hydrocephalus. Brain Pathol. 2004;14(3):317–24.
77. Zhou Q, Anderson DJ. The bHLH transcription factors OLIG2 and OLIG1 couple neuronal and glial subtype specification. Cell. 2002;109(1):61–73.
78. McAllister JP 2nd, Chovan P. Neonatal hydrocephalus mechanisms and consequences. Neurosurg Clin N Am. 1998;9(1):73–93.
79. Duru S, Peiro JL, Oria M, Aydin E, Subasi C, Tuncer C, et al. Successful endoscopic third ventriculostomy in children depends on age and etiology of hydrocephalus: outcome analysis in 51 pediatric patients. Childs Nerv Syst. 2018;34(8):1521–8.
80. Peiro JL, Duru S, Fernandez-Tome B, Peiro L, Encinas JL, Sanchez-Margallo FM, et al. Fetal endoscopic third ventriculostomy is technically feasible in prenatally induced hydrocephalus ovine model. Neurosurgery. 2023;92(6):1303–11.
81. Jones HC, Harris NG, Rocca JR, Andersohn RW. Progressive tissue injury in infantile hydrocephalus and prevention/reversal with shunt treatment. Neurol Res. 2000;22(1):89–96.
82. Del Bigio MR. Neuropathological changes caused by hydrocephalus. Acta Neuropathol. 1993;85(6):573–85.

83. Hale PM, McAllister JP 2nd, Katz SD, Wright LC, Lovely TJ, Miller DW, et al. Improvement of cortical morphology in infantile hydrocephalic animals after ventriculoperitoneal shunt placement. Neurosurgery. 1992;31(6):1085–96.
84. McAllister JP 2nd, Miller JM. Minocycline inhibits glial proliferation in the H-Tx rat model of congenital hydrocephalus. Cerebrospinal Fluid Res. 2010;7:7.
85. Gu C, Hao X, Li J, Hua Y, Keep RF, Xi G. Effects of minocycline on epiplexus macrophage activation, choroid plexus injury and hydrocephalus development in spontaneous hypertensive rats. J Cereb Blood Flow Metab. 2019;39(10):1936–48.
86. Juul SE, Pet GC. Erythropoietin and neonatal neuroprotection. Clin Perinatol. 2015;42(3):469–81.
87. Foerster P, Daclin M, Asm S, Faucourt M, Boletta A, Genovesio A, et al. mTORC1 signaling and primary cilia are required for brain ventricle morphogenesis. Development. 2017;144(2):201–10.
88. Iwasawa E, Brown FN, Shula C, Kahn F, Lee SH, Berta T, et al. The anti-inflammatory agent bindarit attenuates the impairment of neural development through suppression of microglial activation in a neonatal hydrocephalus mouse model. J Neurosci. 2022;42(9):1820–44.
89. Duy PQ, Rakic P, Alper SL, Butler WE, Walsh CA, Sestan N, et al. Brain ventricles as windows into brain development and disease. Neuron. 2022;110(1):12–5.
90. Duy PQ, Timberlake AT, Lifton RP, Kahle KT. Molecular genetics of human developmental neurocranial anomalies: towards "precision surgery." Cereb Cortex. 2023;33(6):2912–8.

Publisher's Note